

Interactive comment on “Northern Hemisphere storminess in the Norwegian Earth System Model (NorESM1-M)” by E. M. Knudsen and J. E. Walsh

E. M. Knudsen and J. E. Walsh

erlend.knudsen@gfi.uib.no

Received and published: 29 February 2016

We thank the anonymous reviewer for his/her suggestions on the manuscript. With the changes explained below, we feel that the paper is strengthened compared to its first submission.

In the following, we go through each comment by the reviewers and explain our choices of changes in accordance to these. Where changes to the text in the manuscript are made, the relevant paragraph is reproduced from the .pdf manuscript to this .docx response, with changes written in [brackets].

Please also see the comment response supplement (gm-2014-227-supplement.pdf), providing the response by the authors to the reviewers in an easier visual version.

C3837

— a) Sea ice retreat and impact on extratropical cyclone causality —

Please see Table 1.

Added new 6th paragraph in 1 Introduction (new text in [brackets]):

[The impacts of a warming climate on high-latitude storms are difficult to anticipate. Both models undergo Arctic-amplified warming at low levels associated with significant loss of sea ice cover in the 21st century simulations examined here. On the one hand, the increased surface fluxes of heat and moisture might be expected to fuel more and stronger storms. On the other hand, the polar amplification decreases the low-level meridional temperature gradients, reducing the potential for storm activity. Nevertheless, because upper-level temperatures show greater increases in the tropics than in the Polar Regions, upper-level meridional temperature gradients actually increase (Harvey et al., 2015). Hence, the net effect on baroclinicity cannot be simply related to baroclinic disturbances such as extratropical cyclones (Ulbrich et al., 2009). Moreover, the Arctic amplification affects the variability of the jet stream, which is directly linked to the vertically integrated meridional temperature gradient via the thermal wind equation. Barnes and Screen (2015) provide a diagnostic assessment of these connections. Here, the model set-up implies that impacts of Arctic warming, sea ice loss and changes in surface fluxes and temperature gradients are implicit in our results.]

Change of 1st bullet point in 4 Conclusions (changes in [brackets]):

The ongoing and projected retreat of sea ice is greatest in autumn, [creating the potential for increased fluxes of sensible and latent heat to from the surface to the atmosphere during these months].

New references:

Barnes, E. and Screen, J.: The impact of Arctic warming on the midlatitude jet-stream: Can it? Has it? Will it?, WIREs Clim. Change, 6, 277–286, doi:10.1002/wcc.337, 2015.

Harvey, B., Shaffrey, L., and Woollings, T.: Deconstructing the climate change re-

C3838

sponse of the Northern Hemisphere wintertime storm tracks, *Clim. Dynam.*, 45, 2847–2860, doi:10.1007/s00382-015-2510-8, 2015.

Ulbrich, U., Leckebusch, G., and Pinto, J.: Extra-tropical cyclones in the present and future climate: a review, *Theor. Appl. Climatol.*, 96, 117–131, doi:10.1007/s00704-008-0083-8, 2009.

— b) Linear scaling with strength of scenario and time —

We agree with the reviewer in that results for RCP4.5 and 2037-2063 should be included in the paper. However, we consider these results secondary to those in the original version of the manuscript. Hence, we have added the results in figures in the Appendix.

Please note that since Figs. A-E are given in the Appendix and not the main body of the manuscript, none of these figures shows significant change or p-values indicating significant change relative to the historical time period for future time periods and scenarios. We believe that Figs. A-E are more compelling without the overlay of the additional information, which complicates the visual presentation of the results.

Added section Appendix B: Additional figures (new text in [brackets]):

<Fig_A.pdf>

[Figure A. Sea ice concentration (a), (f) averages for SOND 1979-2005 and (b), (c), (d), (e), (g), (h), (i), (j) changes in average over various time periods and scenarios relative to 1979– 2005 in NorESM (upper row) and CCSM (lower row). The time periods and scenarios are (b), (g) RCP4.5 2037-2063 – 1979-2005, (c), (h) RCP8.5 2037–2063 – 1979-2005, (d), (i) RCP4.5 2074-2100 – 1979-2005 and (e), (j) RCP8.5 2074-2100 – 1979-2005.]

<Fig_B.pdf>

[Figure B. Sea level pressure (a), (f) averages for SOND (a), (f) 1979-2005 and (b),

C3839

(c), (d), (e), (g), (h), (i), (j) changes in average over various time periods and scenarios relative to 1979– 2005 in NorESM (upper row) and CCSM (lower row). The time periods and scenarios are (b), (g) RCP4.5 2037-2063 – 1979-2005, (c), (h) RCP8.5 2037–2063 – 1979-2005, (d), (i) RCP4.5 2074-2100 – 1979-2005 and (e), (j) RCP8.5 2074-2100 – 1979-2005.]

<Fig_C.pdf>

[Figure C. Track density (a), (f) averages for SOND (a), (f) 1979-2005 and (b), (c), (d), (e), (g), (h), (i), (j) changes in average over various time periods and scenarios relative to 1979– 2005 in NorESM (upper row) and CCSM (lower row). The time periods and scenarios are (b), (g) RCP4.5 2037-2063 – 1979-2005, (c), (h) RCP8.5 2037–2063 – 1979-2005, (d), (i) RCP4.5 2074-2100 – 1979-2005 and (e), (j) RCP8.5 2074-2100 – 1979-2005.]

<Fig_D.pdf>

[Figure D. Mean intensity (a), (f) averages for SOND (a), (f) 1979-2005 and (b), (c), (d), (e), (g), (h), (i), (j) changes in average over various time periods and scenarios relative to 1979– 2005 in NorESM (upper row) and CCSM (lower row). The time periods and scenarios are (b), (g) RCP4.5 2037-2063 – 1979-2005, (c), (h) RCP8.5 2037–2063 – 1979-2005, (d), (i) RCP4.5 2074-2100 – 1979-2005 and (e), (j) RCP8.5 2074-2100 – 1979-2005. Regions with track density below 0.5 no. density (month)–1 (106 km2)–1 in the historical time period are shaded white.]

<Fig_E.pdf>

[Figure E. Precipitation (a), (f) averages for SOND (a), (f) 1979-2005 and (b), (c), (d), (e), (g), (h), (i), (j) changes in average over various time periods and scenarios relative to 1979– 2005 in NorESM (upper row) and CCSM (lower row). The time periods and scenarios are (b), (g) RCP4.5 2037-2063 – 1979-2005, (c), (h) RCP8.5 2037–2063 – 1979-2005, (d), (i) RCP4.5 2074-2100 – 1979-2005 and (e), (j) RCP8.5 2074-2100 –

C3840

1979-2005.]

Change of 1st paragraph and added new 2nd paragraph in 3 Results and discussion (changes in [brackets]):

In the following, parameters representing storminess are presented. While Sect. 3.1 compares the representations of NorESM and CCSM to ERA-I, Sect. 3.2 shows the expected changes of these parameters towards the end of the century, as projected by NorESM and CCSM. Only the 2074–2100 time period following the RCP8.5 scenario is shown here because of the near linear scaling of changes in sea ice, SLP, [track density, mean intensity] and precipitation with strength of scenario (RCP4.5 and RCP8.5) and time (1979–2005 to 2037–2063 and 2074–2100) in our results [(Table 1 and Figs. A to E)]. Hence, we consider the 2037–2063 time period to be an intermediate state between the historical and 2074–2100 periods, and the RCP4.5 scenario to be mid-way to the RCP8.5 scenario.

[While the scaling appear more distinct for sea ice, SLP and precipitation, Figs. C and D show signs of similar behaviour for storm frequency and intensity. This is partly in contrast to Catto et al. (2011). Using the HiGEM high-resolution model, they found northeastward shift of the North Atlantic storm track for the intermediate scenario only. In our results, the northeastward shift gets stronger with scenario and time in NorESM (Figs. Ca to Ce and Figs. Da to De). In CCSM, the North Atlantic storm track generally weakens with scenario and time (Figs. Cf to Cj and Figs. Df to Dj). Overall, signals strengthen with scenario and time in both models. These results extend those of Zappa et al. (2013b), who found mean response generally larger, but also more diverging, for RCP8.5 than RCP4.5 in 19 CMIP5 models (not including CCSM).]

Change of 3rd bullet point in 4 Conclusions (changes in [brackets]):

[For the two models (with one ensemble member each)], the projected changes in storm intensity (as well as sea ice, SLP and precipitation) appear to scale generally linearly with the RCP value of the forcing scenario and with time through the 21st

C3841

century.

New references:

Catto, J., Shaffrey, L., and Hodges, K.: Northern Hemisphere extratropical cyclones in a warming climate in the HiGEM high-resolution climate model, *J. Climate*, 24, 5336–5352, doi:10.1175/2011JCLI4181.1, 2011.

Zappa, G., Shaffrey, L., Hodges, K., Sansom, P., and Stephenson, D.: A multimodel assessment of future projections of North Atlantic and European extratropical cyclones in the CMIP5 climate models*, *J. Climate*, 26, 5846–5862, doi:10.1175/JCLI-D-12-00573.1, 2013b.

— c) Causality between changes in SLP, sea ice and storm tracks —

Please see Figs. 5, 6, A, Ce and Cj, 1st-2nd paragraph in 3.2.1 Sea level pressure, 3rd paragraph in 3.2.3 Mean intensity with references therein. Please also see a) Sea ice retreat and impact on extratropical cyclone causality above and 15: Poleward storm track shift in NorESM and CCSM below.

Change of 4th bullet point in 4 Conclusions (changes in [brackets]):

A significant projected decrease of the SLP over the Arctic Ocean during the 21st century [appears to be] partly a consequence of the diminishing sea ice cover on the same time scales. [These changes are consistent with increased heating of the lower troposphere over areas of sea ice loss, resulting in increased thicknesses in the lower troposphere, and increased geopotential heights and mass divergence aloft. Accordingly, sea level pressures] are projected to [decrease over the Arctic Ocean and] increase farther south, significantly over the North Atlantic Ocean, [coinciding] with [reduced midlatitude] storm [track activity].

— d) Projected changes in mean intensity —

Please see Table 2, Figs. 7, De and Dj and 1st + 3rd paragraph in 3.2.3 Mean intensity.

C3842

Change of 5th bullet point in 4 Conclusions (changes in [brackets]):

[Cyclones are generally expected to weaken over midlatitudes and strengthen over high-latitudes, although this is more apparent for September than December. The intensification is especially marked in areas of sea ice retreat, where cyclones foster from heat fluxes into the atmosphere, latent heat release and reduced friction.]

— e) High-latitude precipitation increase, storm intensification, sea level rise, sea ice loss and vulnerability —

Please see Table 2, Figs. 7, 8 and A and 4th paragraph in 1 Introduction with references therein.

The first sentence, “Autumn precipitation is projected to increase significantly across the entire high-latitudes”, refers to total precipitation, not cyclone-related precipitation exclusively.

The second sentence, “Together with the projected increases in storm intensity and sea level and the loss of sea ice, this increase implies a greater vulnerability to coastal flooding and erosion, especially in the Alaskan region”, refers to Table 2 and Fig. 7 (storm intensity), Table 1 and Fig. A (sea ice) and references to previous work (sea level, coastal flooding and erosion).

Change of 3rd paragraph in 1 Introduction (changes in [brackets]):

Analyses of observational data have produced mixed results on trends of high-latitude storminess. In earlier studies, Zhang et al. (2004) found an increase of Arctic cyclone activity, while McCabe et al. (2001) reported northward shifts of storm tracks over the Northern Hemisphere (NH) over the last several decades of the 20th century. Wang et al. (2006) detected a northward shift of cyclone activity, primarily during winter, over Canada during 1953–2002, and this meridional shift was confirmed more generally in a more recent study by the same group (Wang et al., 2013). The recent U.S. National Climate Assessment (Melillo et al., 2014) points to a poleward shift of storm tracks

C3843

over the United States during recent decades. However, Mesquita et al. (2010) found that temporal trends of cyclones in the North Pacific Ocean have generally been weak over the 60-year period ending 2008. The U.S. Global Change Research Program (Karl et al., 2009) points to an increase of storminess on the northern Alaskan coast and to associated risks of flooding and coastal erosion [along with expected sea level rise]. Since any increases of coastal flooding and erosion are also related to retreating sea ice, [storms in coastal areas of the Arctic can pose increasing risks regardless of whether storm activity is changing].

— f) Study limitations, contributions and future work needed —

Change of 6th paragraph in 2 Data sets and methods (changes in [brackets]):

Only one ensemble member of each model (NorESM: r1i1p1, CCSM: r6i1p1) is examined in the present study because only these ensemble members meet our required criteria for temporal resolution (6-hourly output is needed for cyclone tracking) and choice of scenarios. [Because of this data limitation there is only a thin base for overall evaluation of storminess in CMIP5 models. However, we use multidecadal time slices in order to minimize the effects of internal variations, which account for differences across ensemble members of simulations by any one model. Moreover,] Walsh et al. (2008) found that the spread within ensemble members of a single model is much smaller than inter-model spread when Arctic-averaged temperatures are compared.

Change of 1st paragraph 3 Results and discussion (changes in [brackets]):

In the following, parameters representing storminess are presented. While Sect. 3.1 compares the representations of NorESM and CCSM to ERA-I, Sect. 3.2 shows the expected changes of these parameters towards the end of the century, as projected by NorESM and CCSM. Only the 2074–2100 time period following the RCP8.5 scenario is shown here because of the near linear scaling of changes in sea ice, SLP, [track density, mean intensity] and precipitation with strength of scenario (RCP4.5 and RCP8.5) and time (1979–2005 to 2037–2063 and 2074–2100) in our results [(Table 1 and Figs. A

C3844

to E)]. Hence, we consider the 2037–2063 time period to be an intermediate state between the historical and 2074–2100 periods, and the RCP4.5 scenario to be mid-way to the RCP8.5 scenario.

Please see Figs. A-E and — b) Linear scaling with strength of scenario and time — above.

— 1: Data set comparison and benchmarks —

This special issue of Geoscientific Model Development is on the NorESM. Hence, the main aim of the paper is a validation of storminess simulated by NorESM. This is done by a comparison to the reanalysis data set ERA-I for the historical time period (1979-2005). However, we also included the CMIP5 model CCSM as this model has many of the same components as NorESM. Thus, both ERA-I and CCSM provide benchmarks for comparison to NorESM.

Change of 5th paragraph in 1 Introduction (changes in [brackets]):

Global climate models are arguably the best tools for identifying externally forced signals [(greenhouse gases and aerosols)] in storm activity. In this study, we seek to validate the storm track components of two state-of-the-art global climate models over midlatitudes and high-latitudes of the NH. This is done through a comparison to a reanalysis data set. The models are the Norwegian Earth System Model version 1 with intermediate resolution (NorESM1-M) and the Community Climate System Model version 4 (CCSM4). The simulations examined here were performed as part of the Coupled Model Intercomparison Project phase 5 (CMIP5[; Taylor et al., 2012]). After assessing the models' ability to capture the primary cyclone characteristics over a recent historical period, we compare the future changes of [high- and midlatitude] storms through the late 21st century. The primary metrics of storm activity will be frequency (track density) and intensity. [This evaluation is both a comparison between the time periods for each model and a model intercomparison on diverging changes towards the late 21st century.] The primary metrics of storm activity [here are] frequency (track

C3845

density) and intensity [(mean intensity)].

— 2: Polar amplification and meridional baroclinicity —

Removal of 3rd paragraph, change of 5th paragraph and added new 6th paragraph in 1 Introduction (changes in [brackets]):

Global climate models are arguably the best tools for identifying externally forced signals [(greenhouse gases and aerosols)] in storm activity. In this study, we seek to validate the storm track components of two state-of-the-art global climate models over midlatitudes and high-latitudes of the NH. This is done through a comparison to a reanalysis data set. The models are the Norwegian Earth System Model version 1 with intermediate resolution (NorESM1-M) and the Community Climate System Model version 4 (CCSM4). The simulations examined here were performed as part of the Coupled Model Intercomparison Project phase 5 (CMIP5[; Taylor et al., 2012]). After assessing the models' ability to capture the primary cyclone characteristics over a recent historical period, we compare the future changes of [high- and midlatitude] storms through the late 21st century. The primary metrics of storm activity will be frequency (track density) and intensity. [This evaluation is both a comparison between the time periods for each model and a model intercomparison on diverging changes towards the late 21st century.] The primary metrics of storm activity [here are] frequency (track density) and intensity [(mean intensity)].

[The impacts of a warming climate on high-latitude storms are difficult to anticipate. Both models undergo Arctic-amplified warming at low levels associated with significant loss of sea ice cover in the 21st century simulations examined here. On the one hand, the increased surface fluxes of heat and moisture might be expected to fuel more and stronger storms. On the other hand, the polar amplification decreases the low-level meridional temperature gradients, reducing the potential for storm activity. Nevertheless, because upper-level temperatures show greater increases in the tropics than in the Polar Regions, upper-level meridional temperature gradients actually increase

C3846

(Harvey et al., 2015). Hence, the net effect on baroclinicity cannot be simply related to baroclinic disturbances such as extratropical cyclones (Ulbrich et al., 2009). Moreover, the Arctic amplification affects the variability of the jet stream, which is directly linked to the vertically integrated meridional temperature gradient via the thermal wind equation. Barnes and Screen (2015) provide a diagnostic assessment of these connections. Here, the model set-up implies that impacts of Arctic warming, sea ice loss and changes in surface fluxes and temperature gradients are implicit in our results.]

New references:

Barnes, E. and Screen, J.: The impact of Arctic warming on the midlatitude jet-stream: Can it? Has it? Will it?, *WIREs Clim. Change*, 6, 277–286, doi:10.1002/wcc.337, 2015.

Harvey, B., Shaffrey, L., and Woollings, T.: Deconstructing the climate change response of the Northern Hemisphere wintertime storm tracks, *Clim. Dynam.*, 45, 2847–2860, doi:10.1007/s00382-015-2510-8, 2015.

Taylor, K., Stouffer, R., and Meehl, G.: An overview of CMIP5 and the experiment design, *B. Am. Meteorol. Soc.*, 93, 485–498, doi:10.1175/BAMS-D-11-00094.1, 2012.

Ulbrich, U., Leckebusch, G., and Pinto, J.: Extra-tropical cyclones in the present and future climate: a review, *Theor. Appl. Climatol.*, 96, 117–131, doi:10.1007/s00704-008-0083-8, 2009.

— 3: CCSM description —

Change of 1st + 5th paragraph in 2 Data sets and methods (changes in [brackets]):

The present study uses two global climate models, NorESM1-M and CCSM4, both of which are coupled atmosphere-ocean-land-sea ice models. In keeping with the theme of this special issue, we emphasize NorESM1-M and its simulations. The output of CCSM4, which has somewhat finer resolution, is also examined since its storm simulations can serve as a benchmark for NorESM1-M. The following is a more complete description of NorESM1-M. [Sentence deleted.]

C3847

CCSM4 has twice the horizontal resolution of NorESM, with $1.25^\circ \times 0.9^\circ$ horizontal resolution and 26 vertical layers. [It is developed at UCAR and maintained by NCAR. Described in more detail by Gent et al. (2011), CCSM4 consists of five geophysical models: atmosphere (Community Atmosphere Model; CAM4), land (Community Land Model; CLM4), ocean (Parallel Ocean Program; POP2), land ice (GLC), sea ice (Los Alamos Sea Ice Model/Community Ice CodE; CICE4), and a coupler (CPL7) that coordinates the models and sends information between them.] de Boer et al. (2012) and other accompanying papers in the same CCSM4 special issue of the *Journal of Climate* assess the performance of CCSM4. For the remainder of this paper, CCSM4 will be denoted as CCSM for brevity. Apart from differences in the realizations, [systematic] divergence between the two models [highlights] the role of the ocean, sea ice and atmospheric chemistry in the climate system with other model components being similar.

— 4: Data set limitations —

We agree with the reviewer that the limited data is a thin base for evaluation. Nevertheless, as the main focus in this special issue is NorESM, we argue that the evaluation base is adequate for its purpose.

Change of 6th paragraph in 2 Data sets and methods (changes in [brackets]):

Only one ensemble member of each model (NorESM: r1i1p1, CCSM: r6i1p1) is examined in the present study because only these ensemble members meet our required criteria for temporal resolution (6-hourly output is needed for cyclone tracking) and choice of scenarios. [Because of this data limitation there is only a thin base for overall evaluation of storminess in CMIP5 models. However, we use multidecadal time slices in order to minimize the effects of internal variations, which account for differences across ensemble members of simulations by any one model. Moreover,] Walsh et al. (2008) found that the spread within ensemble members of a single model is much smaller than inter-model spread when Arctic-averaged temperatures are compared.

C3848

Change of 1st paragraph and added new 2nd paragraph in 4 Conclusions (changes in [brackets]):

In this study, we have used a vorticity-based storm-tracking algorithm to analyse changes in metrics of storminess in [high- and midlatitudes] through 2100 in the NorESM1-M global climate model. The main findings obtained from NorESM1-M are generally supported by the results obtained from a second model, CCSM4, which was examined for comparison purposes. [The two models were also compared to the reanalysis data set ERA-Interim for the historical time period. Results are based on only one ensemble member for each model due to the required tracking method criteria.]

[The primary findings include the following:]

— 5: T42 cyclone analysis limitations —

T5-T42 filtering is chosen to specifically focus on the synoptic scale cyclones in vorticity whereas the T40-T100 is designed to focus on mesoscale cyclones. Using relative vorticity for identifying and tracking cyclones, T5-T42 will still likely find some of the larger polar lows but not the very small ones. To resolve the smaller polar lows, Zappa et al. (2014b) and Yanase et al. (2016, *Climatology of polar lows over the Sea of Japan using the JRA-55 reanalysis*, *J. Climate*, 29, 419-437) found T40-T100 to work quite well in the Nordic Seas region and the Sea of Japan, respectively.

In this study, the choice of T5-T42 filtering follows from the data set resolutions. Neither NorESM nor CCSM are of resolutions capable of capturing all polar lows or mesoscale cyclones.

Change of 13th paragraph in 2 Data sets and methods (changes in [brackets]):

The ζ field at moderate to high resolution can nevertheless be very noisy. Hence, to allow the same spatial synoptic scales to be identified in the three data sets, the analysis is performed at a spectral resolution of T42 on a Gaussian grid. Additionally, planetary scales with wave numbers below 5 and above 42 are removed to focus on

C3849

the synoptic variability. [This follows from the data set resolutions and allows some, but not all, polar lows to be resolved (Zappa et al., 2014b).] Finally, criteria regarding their displacement distance (minimum 1000 km) and lifetime (minimum 2 days) are set. Only cyclones (not anticyclones) are considered.

New references:

Zappa, G., Shaffrey, L., and Hodges, K.: Can polar lows be objectively identified and tracked in the ECMWF operational analysis and the ERA-Interim reanalysis?, *Mon. Weather Rev.*, 142, 2596–2608, doi:10.1175/MWR-D-14-00064.1, 2014b.

— 6: Near-linear scaling with strength of scenario and time —

Please see — b) Linear scaling with strength of scenario and time — above.

— 7: SLP and storminess —

Change of 1st paragraph in 3.1.1 Sea level pressure (changes in [brackets]):

SLP [variations are indirect measures of] large-scale storminess. [Pressure gradients in space and pressure changes for a particular point in time both provide indications of storm activity. The] activity generally increases with decreasing SLP as cyclones lower the SLP of a region as they track through [(Trenberth et al., 2007, and references therein)].

New references:

Trenberth, K., Jones, P., Ambenje, P., Bojariu, R., Easterling, D., Klein Tank, A., Parker, D., Rahimzadeh, F., Renwick, J., Rusticucci, M., Soden, B., and Zhai, P.: Observations: surface and atmospheric climate change. In: *Climate Change 2007: The Physical Science Basis. Contribution of Working Group I to the Fourth Assessment Report of the Intergovernmental Panel on Climate Change*, Tech. rep., Intergovernmental Panel on Climate Change (IPCC), Cambridge, United Kingdom and New York, USA, 2007.

— 8: CCSM SLP bias and track density distribution —

C3850

Please see Fig. 6 in DeWeaver and Bitz (2006) and Fig. 4 in de Boer et al (2012).

Change of 5th paragraph in 3.1.1 Sea level pressure (changes in [brackets]):

The substantial SLP bias in CCSM was also noted by DeWeaver and Bitz (2006), who compared the two resolutions T42 and T85 of CCSM3 (CCSM version 3) to the National Centers for Environmental Prediction (NCEP)/NCAR reanalysis. [CCSM3 simulated pressures that were too low for the Aleutian and Icelandic Lows, but with the largest SLP anomalies located over the Beaufort Sea.] They found the bias to be more pronounced in the higher resolution, and ascribed this deficiency to the model's inability to simulate the Beaufort High in autumn, winter and spring. de Boer et al. (2012) showed that this same bias persists in CCSM4.

Change of 4th paragraph in 3.1.2 Track density (changes in [brackets]):

The signal in CCSM offers an additional explanation to the large-scale background SLP [biases across the main storm tracks] discussed in Sect. 3.1.1. [As] more cyclones are resolved in CCSM compared to ERA-I (Table 2), a particular grid point in the storm track [undergoes] low SLP for more time steps, understandably dependent on the cyclone strength. [For regions of the main storm tracks, this can lower the SLP temporal mean.] This is indicated by the anomalous low SLPs [over the poleward-shifted North Atlantic and North Pacific storm tracks (Figs. 1c and 2c). The reason(s) why] CCSM gives more cyclones than ERA-I in the first place is [(are)] unknown, but might reside in its distribution of sea surface temperature or sea ice, or of different parameterization, e.g., for convection.

Please note that Figs. 1-4 have been updated to show differences between the two models to ERA-I rather than separate means of the three data sets. Hence, Figs. 1-4 (b) and (c) now shows NorESM – ERA-I and CCSM – ERA-I instead of NorESM and CCSM historical time period means, respectively. NorESM and CCSM historical means are shown in Figs. A-E (a) and (f).

C3851

Update of Fig. 1 (caption changes in [brackets]):

<Fig_1.pdf>

Figure 1. [Sea level pressure average] for SOND 1979–2005 in (a) ERA-I [and bias of (b) NorESM and (c) CCSM relative to ERA-I. Alternating black and white dots in (b) and (c) mark regions of significant bias at a 95 % confidence level.]

Update of Fig. 2 (caption changes in [brackets]):

<Fig_2.pdf>

Figure 2. [Track density average] for SOND 1979–2005 in (a) ERA-I [and bias of (b) NorESM and (c) CCSM relative to ERA-I. Alternating black and white dots in (b) and (c) mark regions where $p < 0.05$ based on 2000 samples.]

Update of Fig. 3 (caption changes in [brackets]):

<Fig_3.pdf>

Figure 3. [Mean intensity average] for SOND 1979–2005 in (a) ERA-I [and bias of (b) NorESM and (c) CCSM relative to ERA-I]. Regions with track density below 0.5 no. density (month)⁻¹ (106 km²)⁻¹ are shaded white. [Alternating black and white dots in (b) and (c) mark regions where $p < 0.05$ based on 2000 samples.]

Update of Fig. 4 (caption changes in [brackets]):

<Fig_4.pdf>

Figure 4. [Precipitation average] for SOND 1979–2005 in (a) ERA-I [and bias of (b) NorESM and (c) CCSM relative to ERA-I. Alternating black and white dots in (b) and (c) mark regions of significant bias at a 95 % confidence level.]

— 9: Mean intensity shift vs. bias over North America and Eurasia —

We have rephrased the relevant paragraph (2nd paragraph in 3.1.3 Mean intensity).

C3852

Change of 2nd paragraph in 3.1.3 Mean intensity (changes in [brackets]):

Corresponding to the [general poleward shift] of the SLP [minima and track density maxima along the two main storm tracks relative to ERA-I (Figs. 1 and 2), NorESM and CCSM have too low mean intensities over the North Atlantic and North Pacific oceans (Figs. 3b and 3c). Conversely, as for track density, positive biases are found over large swaths of Eurasia and western North America, indicating lower contrasts between regions of high and low cyclonic activity in the models compared to ERA-I (Figs. 2b, 2c, 3b and 3c).]

— 10: Zappa et al. (2013a) discussion —

Change of 4th paragraph in 3.1.3 Mean intensity (changes in [brackets]):

Our results add to the CMIP5 model underestimation of cyclone intensities in the North Atlantic Ocean in winter and summer compared to ERA-I found by Zappa et al. (2013a). [They attributed this bias to either an incorrect representation of dynamical processes on the spatiotemporal scales of cyclones (e.g., baroclinic conversion, diabatic heating, dissipation) or to biases in the large-scale processes (e.g., flow-orography interaction, tropical convection, radiative forcing) that determine the environment in which the cyclones grow. Here,] Fig. 3 shows that cyclones are generally weaker in the two CMIP5 models NorESM and CCSM [than ERA-I also] in the extended autumn season.

— 11: Precipitation and storminess —

Change of 1st paragraph in 3.1.4 Precipitation (changes in [brackets]):

[In terms of broad-scale pattern, precipitation is positively correlated with storminess, although one cannot say that precipitation is a real measure of storminess. Hawcroft et al. (2012) and Catto et al. (2012) showed the proportion of precipitation associated with extratropical cyclones and fronts, respectively. Only through this type of linkage can a causal relationship be established. In this study, because precipitation per se is not our main focus, we merely point to consistencies between our results and general charac-

C3853

teristics of precipitation vis-à-vis its drivers. For example,] cyclone-dense regions are [generally] characterized by high frontal precipitation, with precipitation reaching [especially] high levels [where] cyclones track into mountainous land [so that precipitation is orographically enhanced].

Change of 2nd paragraph in 3.2.4 Precipitation (changes in [brackets]):

[The reduced precipitation in the eastern North Atlantic Ocean in September coincides with reduced cyclone frequency in CCSM and intensity in both NorESM and CCSM (Figs. 8a and 8b compared to Figs. 6b, 7a and 7b). The correspondence between precipitation and cyclone intensity is consistent with the findings of Zappa et al. (2013b). However, while the changes in storm tracks and precipitation are coherent, this consistency does not prove a causal relationship. The expected drying of the eastern North Atlantic Ocean stems from the poleward migration of the Hadley Cell's downward limb (Kang and Lu, 2012), which is projected to increase dryness in the African-Eurasian region (including the Mediterranean), southwestern North America and northeastern Brazil (Lau and Kim, 2015). The eastern North Atlantic] is projected to warm less than the rest of the NH, with relatively lower humidity [reducing the] potential for increased atmospheric moisture (Stocker et al., 2013). [In December, the changes of precipitation in the eastern North Atlantic are mostly positive and are not strongly related to storm track changes (Figs. 8c and 8d).]

New references:

Catto, J., Jakob, C., Berry, G., and Nicholls, N.: Relating global precipitation to atmospheric fronts, *Geophys. Res. Lett.*, 39, L10 805, doi:10.1029/2012GL051736, 2012.

Hawcroft, M., Shaffrey, L., Hodges, K., and Dacre, H.: How much Northern Hemisphere precipitation is associated with extratropical cyclones?, *Geophys. Res. Lett.*, 39, L24 809, doi:10.1029/2012GL053866, 2012.

Zappa, G., Shaffrey, L., Hodges, K., Sansom, P., and Stephenson, D.: A multimodel

C3854

assessment of future projections of North Atlantic and European extratropical cyclones in the CMIP5 climate models*, *J. Climate*, 26, 5846–5862, doi:10.1175/JCLI-D-12-00573.1, 2013b.

— 12: Comparison of convective, orographic and large-scale precipitation —

Change of 2nd paragraph in 3.1.4 Precipitation (changes in [brackets]):

[Figures 4a, Ea and Ef] show the average pattern of precipitation for NH midlatitudes and high-latitudes over the historical time period. [While climate models generally distinguish convective and non-convective precipitation, their archives do not distinguish frontal and orographic precipitation – two of the primary types of non-convective precipitation. Nevertheless, one can infer that heavy precipitation events in non-mountainous areas have a general association with frontal activity (Kunkel et al. 2012), while precipitation maxima in mountainous areas have a substantial orographic component. Subject to these assumptions, some inferences can be made about the key features that stand out in Fig. 4.] [Sentence moved.]

New references:

Kunkel, K., Easterling, D., Kristovich, D., Gleason, B., Stoecker, L., and Smith, R.: Meteorological causes of the secular variations in observed extreme precipitation events for the conterminous United States, *J. Hydrometeorology*, 13, 1131–1141, doi:10.1175/JHM-D-11-0108.1, 2012.

— 13: Positive AO resemblance and comparison to model results —

Change of 3rd paragraph in 3.2.1 Sea level pressure (changes in [brackets]):

The patterns in Fig. 5 bear resemblance to the positive phase of the Arctic Oscillation (AO). This is indicative of a [stronger, less wavy] jet stream, which steers storms eastwards to the north of their usual paths and leaves midlatitudes with fewer cold air outbreaks than usual (Thompson and Wallace, 2001). [As in other CMIP5 models (Barnes and Polvani, 2013), this pattern is more marked in the North Atlantic compared

C3855

to the North Pacific sector in NorESM and CCSM.]

New references:

Barnes, E. and Polvani, L.: Response of the midlatitude jets, and of their variability, to increased greenhouse gases in the CMIP5 models, *J. Climate*, 26, 7117–7135, doi:10.1175/JCLI-D-12-00536.1, 2013.

— 14: Poleward storm track shift in previous work —

Change of 1st + 5th paragraph in 3.2.2 Track density (changes in [brackets]):

The variability in the North Pacific storm track severely determines the day-to-day weather conditions [downstream] in the coastal regions of western Canada and southern Alaska. The same can be said of the North Sea region from the North Atlantic storm track, [both regions] represented by wet and [stormy] climates [in Figs. 2a, 3a and 4a. This feature explains the choice of regions shown in Fig. 6a. Some earlier studies have indicated poleward shifts of the two main storm tracks in a warmer climate (e.g., Bengtsson et al., 2006, 2009, Fischer-Bruns et al., 2005). If this also holds for NorESM and CCSM, we would expect to see track density reductions in WNA and NWE with corresponding enhancements in BWA and NEE. However, Table 3 shows no clear indications of these shifts.]

According to NorESM and CCSM, fewer cyclones will track along the current main storm tracks in the North Atlantic and North Pacific oceans towards the end of the century (Fig. 6). This explains the 3.9–6.5 % reductions in midlatitudes found in Table 2[, with up to 20.1 % and 21.7 % drops in WNA and NWE activity, respectively (Table 3)]. On the other hand, there [are signals partly indicating more cyclones poleward of this in the two models in Fig. 6].

New references:

Fischer-Bruns, I., von Storch, H., González-Rouco, J., and Zorita, E.: Modelling the variability of midlatitude storm activity on decadal to century time scales, *Clim. Dynam.*,

C3856

Change in Abstract (changes in [brackets]):

Metrics of storm activity in Northern Hemisphere high- and midlatitudes are evaluated from historical output and future projections by the Norwegian Earth System Model (NorESM1-M) coupled global climate model. The European Re-Analysis Interim (ERA-Interim) and the Community Climate System Model (CCSM4), a global climate model of the same vintage as NorESM1-M, provide benchmarks for comparison. The focus is on the autumn and early winter (September through December) [the period when the ongoing and projected Arctic sea ice retreat is greatest]. Storm tracks derived from a vorticity-based algorithm for storm identification are reproduced well by NorESM1-M, although the tracks are somewhat better resolved in the higher-resolution ERA-Interim and CCSM4. The tracks [show indications of shifting] polewards in the future as climate changes under the Representative Concentration Pathway (RCP) forcing scenarios. Cyclones are projected to become generally more intense in the high-latitudes, especially over the Alaskan region, although in some other areas the intensity is projected to decrease. While projected changes in track density are less coherent, there is a general tendency towards less frequent storms in midlatitudes and more frequent storms in high-latitudes, especially the Baffin Bay/Davis Strait region [in September]. Autumn precipitation is projected to increase significantly across the entire high-latitudes. Together with the projected increases in storm intensity and sea level and the loss of sea ice, this increase in precipitation implies a greater vulnerability to coastal flooding and erosion, especially in the Alaskan region. The projected changes in storm intensity and precipitation (as well as sea ice and sea level pressure) scale generally linearly with the RCP value of the forcing and with time through the 21st century.

Added new 3rd-8th paragraphs in 3.2.2 Track density (changes in [brackets]):

[The general reduction in North Pacific cyclones is associated with more cyclones in

C3857

parts of the Bering Sea (Fig. 6). However, no consistent tendency is found for the two models and two months, explaining the highly varying changes for BWA in Table 3 (from -13.4 % to +15.5 %). A comparison to Harvey et al. (2015) reveals that this signal of a poleward shift of the North Pacific storm track was more apparent in CMIP3 models.]

[NorESM projects a stronger northward shift than CCSM in the North Pacific sector (Figs. 6a and 6c compared to Figs. 6b and 6d), although December averages within the chosen regions suggests the opposite (+18.2 % in WNA, -13.4 % in NWE; Table 3). While more cyclones are expected to track through the Bering Strait and into the Arctic Ocean in September, NorESM indicates a more zonal pattern in the North Pacific Ocean for December with a significant increase in a band around 50°N (Figs. 6a and 6c). This pattern is not found in CCSM (Figs. 6b and 6d), which rather projects strong increases along the North American and Siberian Arctic coasts in December (Fig. 6d). The latter feature is mostly a consequence of coinciding enhanced cyclone generation (not shown).]

[Fewer cyclones track across the North Atlantic Ocean overall in both months and models (Fig. 6). NorESM, like the majority of CMIP5 models (Feser et al., 2015, and references therein), project an eastward extension of the North Atlantic storm track (Figs. 6a and 6c). This evolution occurs downstream of an already too zonal storm track compared to the reanalysis (Fig. 2b), with a 10.2 to 12.8 % increase in NWE (Table 3). CCSM too represents the North Atlantic storm track too zonal originally (Fig. 2c), but projects no clear indications of a more zonal storm track towards the end of the 21st century (-21.7 to +1.2 % for NWE in Table 3).]

[No significant changes are found in NEE (Table 3 and Figs. 6a and 6c). Rather, both NorESM and CCSM show weak reductions in NEE track density (-11.6 to -0.8 %; Table 3) associated with enhancements in the Greenland Sea in September (Figs. 6a and 6b). Fig. A reveals that the latter increase coincides with a sea ice retreat in the Greenland Sea over the century. These results follow those of Deser et al. (2000),

C3858

Magnusdottir et al. (2004) and Knudsen et al. (2015), who found storm activity to be very sensitive to the sea ice variations east of Greenland. Moreover, Chen et al. (2015) showed a corresponding sensitivity in synoptic activity here associated with variations in the surface mass balance of the Greenland Ice Sheet.]

[Corresponding to the observed trend found by Sepp and Jaagus (2011), the raised number of cyclones tracking through the Greenland Sea coincides with an increase also in the Labrador Sea and Baffin Bay. While the additional cyclones in these regions are short-lived in CCSM (not shown), they continue polewards (not shown) and add to the projected Arctic Ocean cyclonic activity increase from the Pacific sector in NorESM (Fig. 6a). Nevertheless, this Arctic enhancement is found in September for NorESM alone, and the high-latitude circumglobal changes over the whole season in both models are negligible (-0.8 to +0.3 %; Table 2). This contrasts Harvey et al. (2015), who found a significant decrease in high-latitude storm activity with retreating sea ice edge, thus highlighting the complex interconnections determining synoptic changes in a warmer climate system.]

[Numerous reanalysis studies have shown tendencies of poleward-shifted storm tracks in both the North Atlantic and North Pacific oceans over time (e.g., McCabe et al., 2001, Sepp and Jaagus, 2011, Wang et al., 2006, 2013). Here, only December projections in NorESM resemble similar results. Rather, the general picture of the two main storm tracks in Fig. 6 is more in line with more recent results (e.g., Harvey et al., 2015, Zappa et al., 2013b), with indications of a poleward-shifted North Pacific storm track and eastward-elongated North Atlantic storm track.]

Change of 6th bullet point in 4 Conclusions (changes in [brackets]):

Projected changes in track density are much less coherent, although there is a general tendency towards less frequent storms in midlatitudes and more frequent storms in [certain regions at] high-latitudes. Relatively large increases in frequency are projected [locally] for the Baffin Bay/Davis Strait region [in September].

C3859

New references:

Chen, L., Fettweis, X., Knudsen, E., and Johannessen, O.: Impact of cyclonic and anticyclonic activity on Greenland ice sheet surface mass balance variation during 1980–2013, *Int. J. Climatol.*, doi:10.1002/joc.4565, 2015.

Deser, C., Walsh, J., and Timlin, M.: Arctic sea ice variability in the context of recent atmospheric circulation trends, *J. Climate*, 13, 617–633, doi:10.1175/1520-0442(2000)013<0617:ASIVIT>2.0.CO;2, 2000.

Feser, F., Barcikowska, M., Krueger, O., Schenk, F., Weisse, R., and Xia, L.: Storminess over the North Atlantic and northwestern Europe – A review, *Q. J. Roy. Meteor. Soc.*, 141, 350–382, doi:10.1002/qj.2364, 2015.

Harvey, B., Shaffrey, L., and Woollings, T.: Deconstructing the climate change response of the Northern Hemisphere wintertime storm tracks, *Clim. Dynam.*, 45, 2847–2860, doi:10.1007/s00382-015-2510-8, 2015.

Knudsen, E., Orsolini, Y., Furevik, T., and Hodges, K.: Observed anomalous atmospheric patterns in summers of unusual Arctic sea ice melt, *J. Geophys. Res.-Atmos.*, 120, 2595–2611, doi:10.1002/2014JD022608, 2015.

Magnusdottir, G., Deser, C., and Saravanan, R.: The effects of North Atlantic SST and sea ice anomalies on the winter circulation in CCM3. Part I: Main features and storm track characteristics of the response, *J. Climate*, 17, 857–876, doi:10.1175/1520-0442(2004)017<0857:TEONAS>2.0.CO;2, 2004.

Zappa, G., Shaffrey, L., Hodges, K., Sansom, P., and Stephenson, D.: A multimodel assessment of future projections of North Atlantic and European extratropical cyclones in the CMIP5 climate models*, *J. Climate*, 26, 5846–5862, doi:10.1175/JCLI-D-12-00573.1, 2013b.

— 16: Cyclone lifetime trends in reanalysis and model projections —

C3860

Change of 1st paragraph in 3.2.3 Mean intensity (changes in [brackets]):

Towards the end of the century, cyclones generally weaken over midlatitudes (including the main storm tracks) and strengthen over high-latitudes (Table 2 and Fig. 7). This corresponds to the overall picture in Fig. 6, although the high-latitude amplification is clearer for intensities (Table 2). On the other hand, the weakening in midlatitudes is smaller, with an average 2 % reduction in mean intensity over the domain of the two models compared to 4 % decrease in track density. In other words, while there is a projected decrease in number of storms crossing the North Atlantic and the North Pacific oceans, their strength will not drop proportionally. We propose this feature is a result of the overall warming, where higher temperatures and corresponding increases of atmospheric moisture generally favour stronger cyclones. [Sentence deleted.]

— 17: Model resolution and cyclone metrics representation —

Change of 2nd bullet point in 4 Conclusions (changes in [brackets]):

The models reproduce the observed seasonality of the sea ice loss and the general patterns of sea level pressure (SLP) and cyclone metrics, although the storm tracks (densities) and intensities are somewhat less sharp relative to ERA-I because of the models' coarser resolution. [Sentence deleted.]

— 18: Track density changes in the Baffin Bay/Davis Strait region —

Change in Abstract (changes in [brackets]):

Metrics of storm activity in Northern Hemisphere high- and midlatitudes are evaluated from historical output and future projections by the Norwegian Earth System Model (NorESM1-M) coupled global climate model. The European Re-Analysis Interim (ERA-Interim) and the Community Climate System Model (CCSM4), a global climate model of the same vintage as NorESM1-M, provide benchmarks for comparison. The focus is on the autumn and early winter (September through December) [âĀĤ] the period when the ongoing and projected Arctic sea ice retreat is greatest. Storm tracks derived from

C3861

a vorticity-based algorithm for storm identification are reproduced well by NorESM1-M, although the tracks are somewhat better resolved in the higher-resolution ERA-Interim and CCSM4. The tracks [show indications of shifting] polewards in the future as climate changes under the Representative Concentration Pathway (RCP) forcing scenarios. Cyclones are projected to become generally more intense in the high-latitudes, especially over the Alaskan region, although in some other areas the intensity is projected to decrease. While projected changes in track density are less coherent, there is a general tendency towards less frequent storms in midlatitudes and more frequent storms in high-latitudes, especially the Baffin Bay/Davis Strait region [in September]. Autumn precipitation is projected to increase significantly across the entire high-latitudes. Together with the projected increases in storm intensity and sea level and the loss of sea ice, this increase in precipitation implies a greater vulnerability to coastal flooding and erosion, especially in the Alaskan region. The projected changes in storm intensity and precipitation (as well as sea ice and sea level pressure) scale generally linearly with the RCP value of the forcing and with time through the 21st century.

Change of 6th bullet point in 4 Conclusions (changes in [brackets]):

Projected changes in track density are much less coherent, although there is a general tendency towards less frequent storms in midlatitudes and more frequent storms in [certain regions at] high-latitudes. Relatively large increases in frequency are projected [locally] for the Baffin Bay/Davis Strait region [in September].

Please also note the supplement to this comment:

<http://www.geosci-model-dev-discuss.net/7/C3837/2016/gmdd-7-C3837-2016-supplement.pdf>

Interactive comment on Geosci. Model Dev. Discuss., 7, 8975, 2014.

C3862

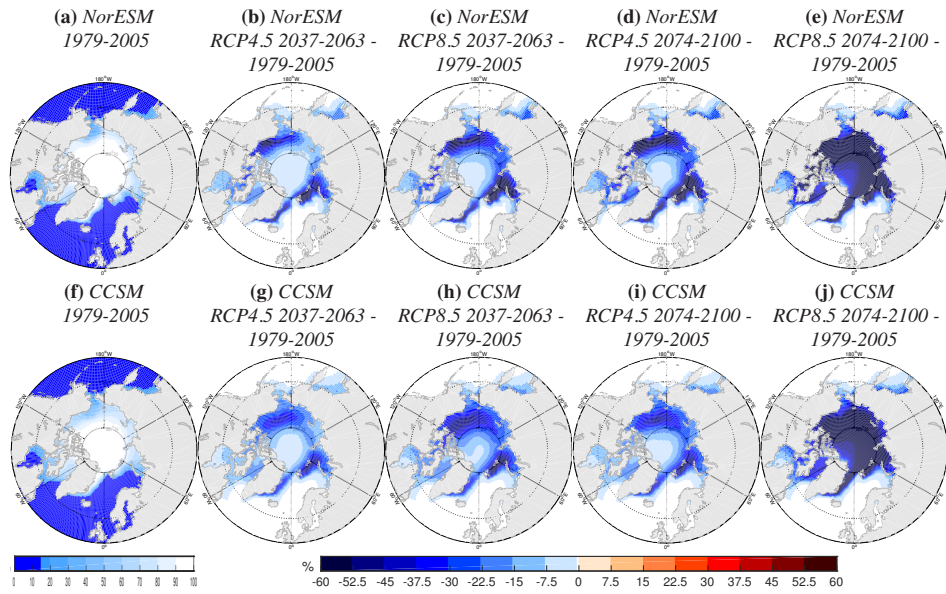


Fig. 1. New Figure A. Please see supplement or — b) Linear scaling with strength of scenario and time — for caption.

C3863

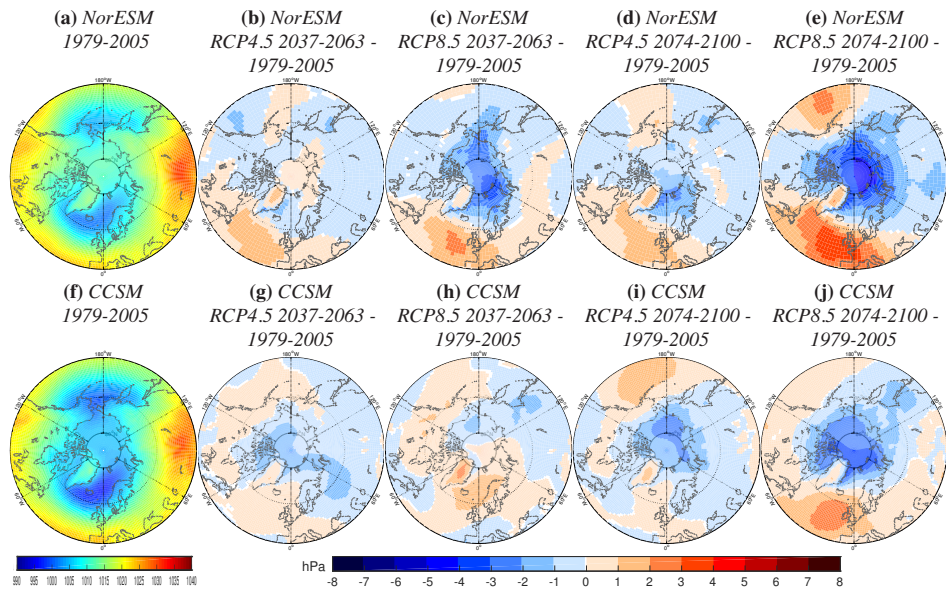


Fig. 2. New Figure B. Please see supplement or — b) Linear scaling with strength of scenario and time — for caption.

C3864

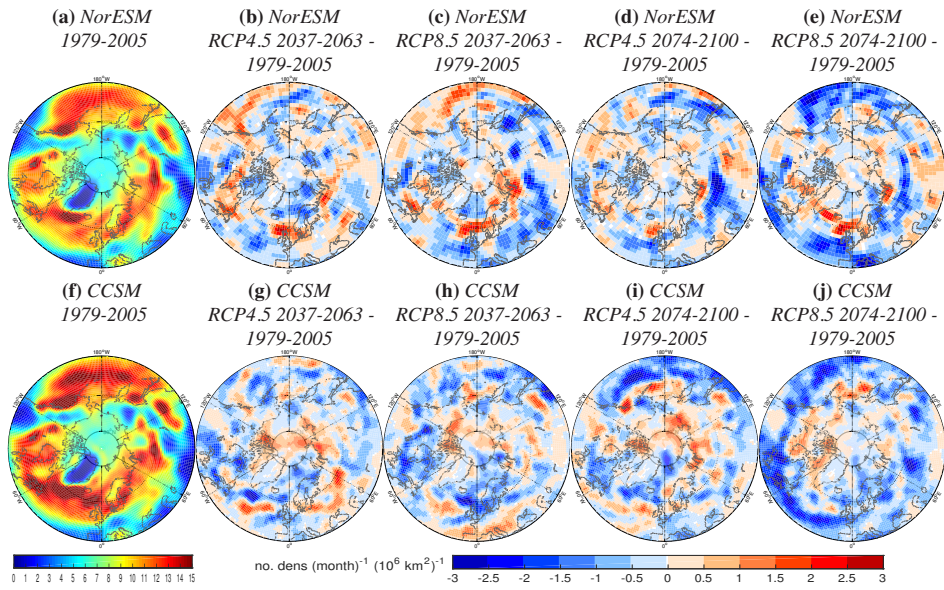


Fig. 3. New Figure C. Please see supplement or — b) Linear scaling with strength of scenario and time — for caption.

C3865

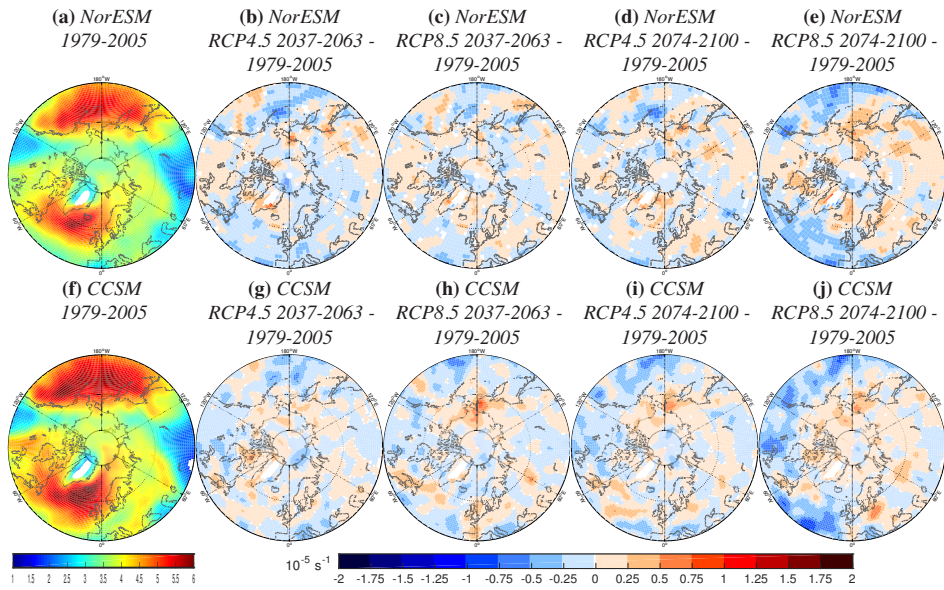


Fig. 4. New Figure D. Please see supplement or — b) Linear scaling with strength of scenario and time — for caption.

C3866

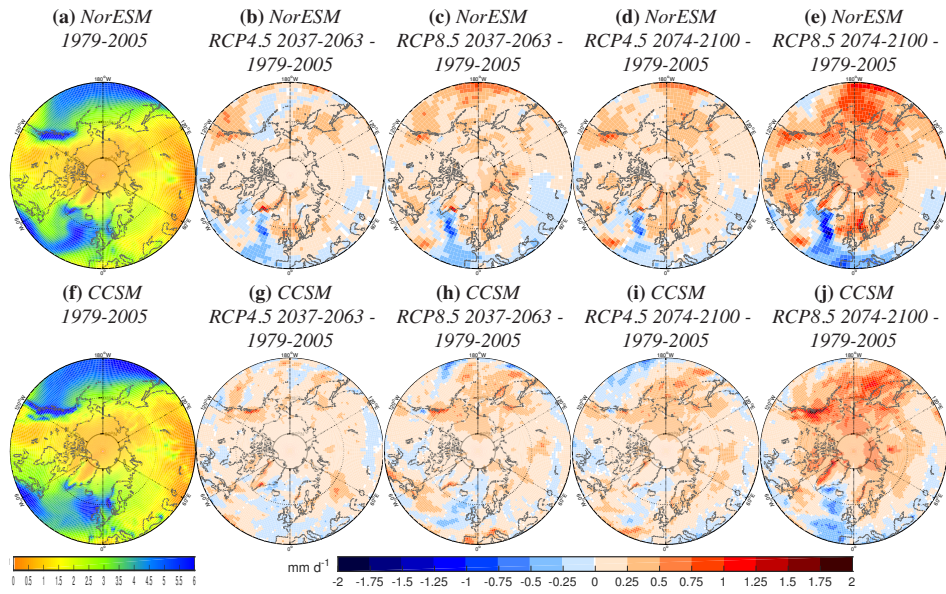


Fig. 5. New Figure E. Please see supplement or — b) Linear scaling with strength of scenario and time — for caption.

C3867

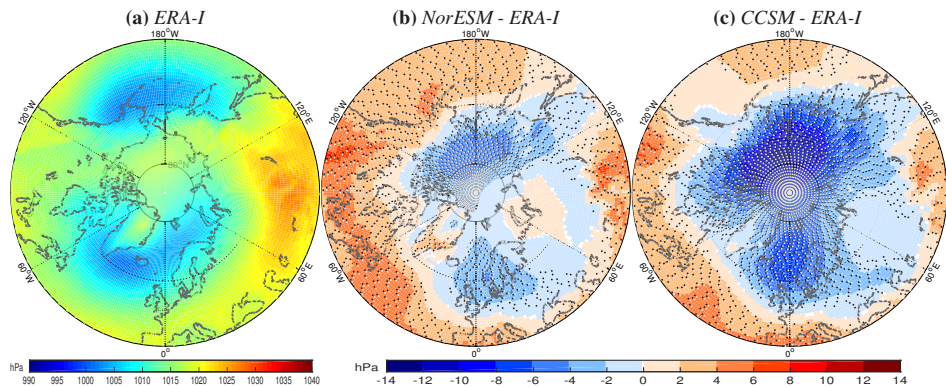


Fig. 6. Changed Figure 1. Please see supplement or — 8: CCSM SLP bias and track density distribution — for caption.

C3868

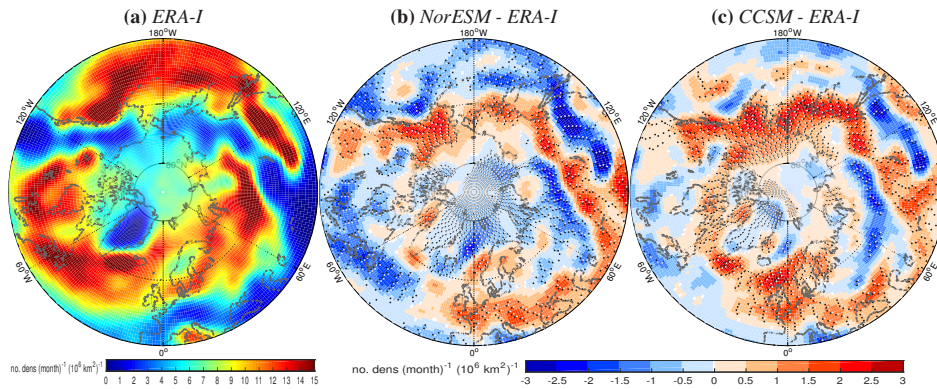


Fig. 7. Changed Figure 2. Please see supplement or — 8: CCSM SLP bias and track density distribution — for caption.

C3869

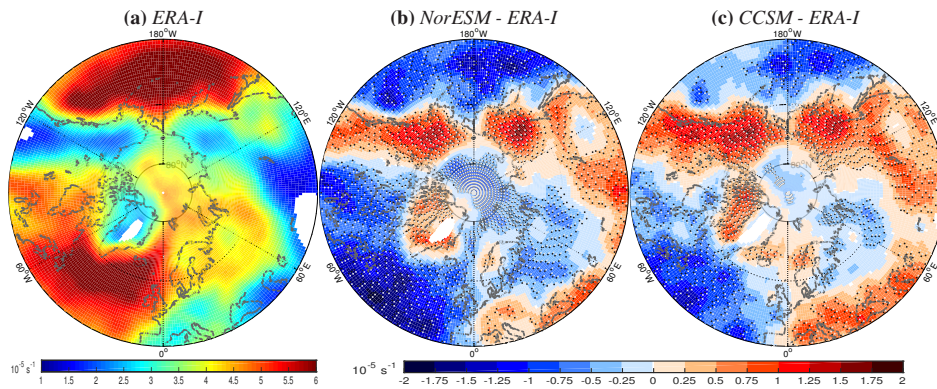


Fig. 8. Changed Figure 3. Please see supplement or — 8: CCSM SLP bias and track density distribution — for caption.

C3870

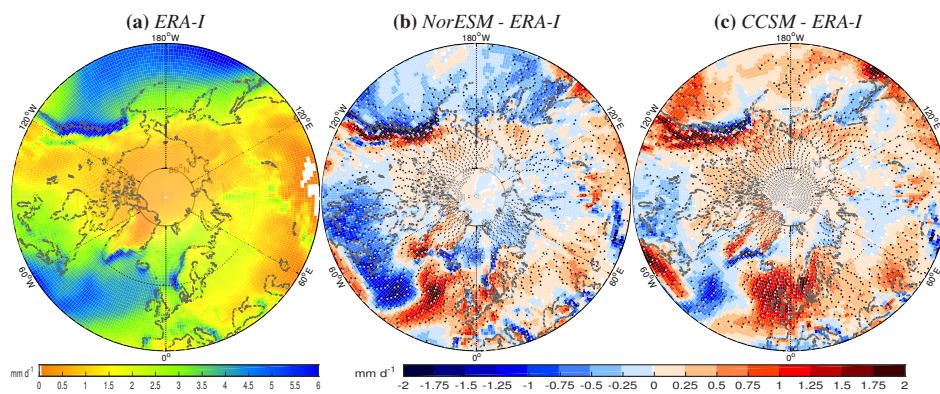


Fig. 9. Changed Figure 4. Please see supplement or — 8: CCSM SLP bias and track density distribution — for caption.